Simple Method for Multi-access Frequency Transfer with Remote Passive Phase Noise Compensation

Shi Luo, Zhibin Zhang, Shun Wu*

Hubei Key Laboratory of Optical Information and Pattern Recognition, Wuhan Institute of Technology, Wuhan 430205, China

In this paper, we demonstrated a star-shaped frequency dissemination system based on fiber optic. By passively eliminating the phase noise at the remote end, we simplified the configuration of the local end. So that the scalability of the system had been improved. In addition, a dual-mixer device was implemented to eliminate the RF leakage caused by the limited isolation of the mixer, which greatly improves the long-term stability of the dissemination system. The relative frequency stability reaches 1.35×10^{-14} at 1 s and 6.32×10^{-17} at 10^4 s over a 50 km fiber link. Our scheme provides a simple method for multi-access frequency transfer, which has great potential in frequency distribution network.

Keywords: Multi-access; frequency transfer; passive compensation; dual-mixer device

1. Introduction

High-precision microwave frequency dissemination technology is extensively applied in areas such as satellite navigation, fundamental physical quantity measurement, radio astronomy, and etc[1-6]. Owing to its low loss, strong anti-interference capabilities, and abundant resources, optical fiber has emerged as an ideal medium for frequency dissemination[7-9]. However, in practical fiber-optic links, additional phase noise can be introduced to the transfer system by external environmental disturbances, such as fluctuations in fiber-optic temperature and mechanical interference. This, in turn, degrades the frequency stability of the received signal. Since the round-trip phase noise compensation method was proposed[10], microwave frequency dissemination has shown an instability level of 10^{-18} for integration time less than 10^4 seconds[11]. Nevertheless, as the number of users grows, the conventional point-to-point transmission method, which relies on end-point noise compensation, is no longer suitable[12-15]. This is because an increase in the number

of users leads to a proportional rise in system complexity at the local end, which, in turn, requires more power to distribute the reference signal to multiple users.

To achieve scalability in frequency transfer, two multi-access strategies were proposed. The first strategy involved recovering the RF modulation signal at any arbitrary point along the fiber link[16-18]. While employing different carrier wavelengths helped suppress backscattering, the inclusion of optical-to-electrical and electrical-to-optical conversion components significantly increased the system's complexity and cost. Moreover, because all users shared the main link, damage to one link could compromise the accurate reception of frequency for the others. The second scheme aimed at enhancing scalability involved the use of branch fiber optical networks with phase noise compensation at each remote end[19-22]. Tree-shaped and star-shaped frequency distribution networks greatly simplified the local configuration and supported the central site to send frequency signals to multiple users in different locations around. However, the use of different carrier wavelengths to distinguish between users introduced group velocity dispersion (GVD) due to the varying propagation speeds of different wavelengths of light in optical fibers. This dispersion effect led to asymmetric phase delays for different wavelengths of light travelling over the same length of fiber. The greater the wavelength difference, the more pronounced the asymmetry in phase delay. To address this issue, Li-jun Wang *et. al.* demonstrated a transmission scheme where the transmission signal was directly looped back to the corresponding link, ensuring that each user employed the same carrier wavelength[23, 24].

In this paper, we proposed and demonstrated a frequency distribution system based on user-side passive noise compensation. By deploying the "dual-mixer technique" at the remote end, phase noise was passively mitigated without the need for active electronic servo feedback. All remote stations shared the carrier of the same wavelength to circumvent the effects of GVD. The system achieved relative frequency stabilities of 1.35×10^{-14} at 1 s and 6.32×10^{-17} at 10^4 s over a 50 km dissemination, marking a two-order-of-magnitude enhancement over systems without the dual-mixer configuration. Experimental findings showed that our frequency

distribution system is resilient to temperature fluctuations. Our approach offers a valuable reference for cost-effective multi-access frequency transfer over short distances.

2. Principle

Figure 1 illustrates the schematic diagram of a system that employs remote noise compensation. The reference signal E_0 is transmitted by intensity-modulating a distributed feedback (DFB) laser operating at a λ_1 and transferred to the remote end. A portion of E_1 is then modulated to the carrier wavelength λ_2 for round-trip dissemination (E_3), while the remaining portion is frequency tripled (E_2) before mixed with E_3. Consequently, the phase noise introduced by fiber-optic can be compensated.

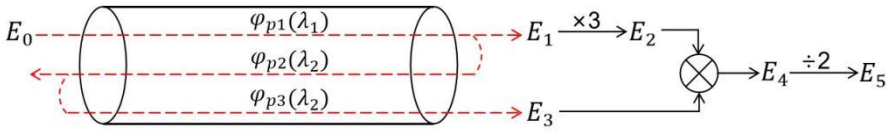

Fig. 1. Principle of the fiber link noise compensation.

Without considering its amplitude, the E_0 is expressed as

$$E_0 = \cos(\omega_0 t + \varphi_0) \tag{1}$$

where ω_0 and φ_0 represent the angular frequency and initial phase of the signal, respectively. The signal E_1 detected at the remote end can be written as

$$E_1 = \cos(\omega_0 t + \varphi_0 + \varphi_{p1}) \tag{2}$$

where φ_{p1} is the phase change induced by the optical fiber during the dissemination. The triple-frequency signal E_2 and the signal E_3 can be expressed as

$$E_2 = \cos(3\omega_0 t + 3\varphi_0 + 3\varphi_{p1}) \tag{3}$$

$$E_3 = \cos(\omega_0 t + \varphi_0 + \varphi_{p1} + \varphi_{p2} + \varphi_{p3}) \tag{4}$$

where φ_{p2} and φ_{p3} are the phase changes induced in the second and third trip. The effect of asymmetric delay can be ignored when the difference between wavelengths λ_1 and λ_2 is small enough, that is, $\varphi_{p1} \approx \varphi_{p2} \approx \varphi_{p3}$. Then E_2 is frequency mixed

with E_3 to produce an intermediate frequency (IF) signal

$$E_4 = \cos(2\omega_0 t + 2\varphi_0) \quad (5)$$

The recovered frequency signal does not include the phase fluctuation term. The compensated transmitted signal E_5 obtained after frequency division can be expressed as

$$E_5 = \cos(\omega_0 t + \varphi_0) \quad (6)$$

which is identical to the reference frequency indicating that the reference frequency is recovered at the remote end.

3. Experimental setup

The schematic diagram of the distribution system is shown in Figure 2. The experiment was carried out indoor where the temperature fluctuated by approximately 3 ℃ throughout the day. The 2.5 GHz reference signal was produced from a signal generator stabilized to a rubidium clock, and then modulated on an optical carrier (λ_1) using a Mach-Zehnder modulator (MZM) for transmission to the remote end. During the experiment, a 50 km single-mode fiber was employed followed by a 5 km dispersion compensation fiber to counteract the dispersion accumulated along the fiber link. At the remote end, the signal carried on λ_1 was split in halves by an optical coupler (OC3). Each portion was optically filtered amplified at λ_1 and λ_2, respectively, before being photodetected by PD1 and PD2. A second optical carrier (λ_2) was transmitted from the remote end back along the same fiber link to mitigate the effects of backscattering. This was achieved by routing the signal through circulator 1 and OC2, thus completing the round-trip transmission before it reached OC3. The wavelengths of the two DFB lasers were 1550.92 nm and 1551.72 nm, corresponding to International Telecommunication Union (ITU) channels C33 and C32, respectively. It is worth mentioning that we split the modulated light by using OC1, with each branch's signal independently transfer over the link. This ensures that the returned signals from different users do not overlap, thus mitigating the impact of group velocity dispersion. In our scheme, using 1×3 OC, we can realize three 50 km

fiber links simultaneously. In addition, we can choose the splitting ratio of the OC1 based on the distance between different user and the local end.

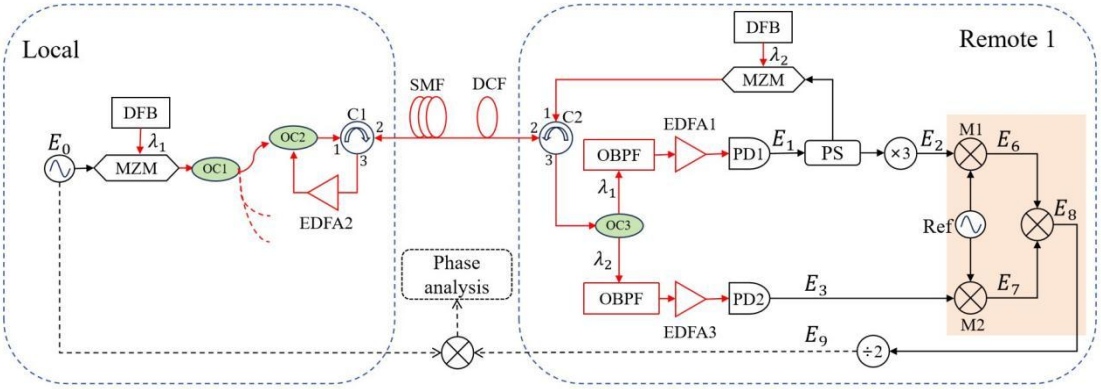

Fig. 2. Experimental setup for the frequency distribution system. MZM: Mach-Zehnder modulator. DFB: distributed feedback laser. OC: optical coupler. C: circulator. OBPF: optical bandpass filter. PD: photodetector. M: mixer. PS: power splitter. ×3: frequency tripler. ÷2: frequency divider. EDFA: erbium-doped fiber amplifier. SMF: single-mode fiber. DCF: dispersion compensation fiber. Ref: RF reference.

Due to the mixer's limited RF isolation, the signal E_4 depicted in Fig. 1 contained frequency harmonics of the input signal[25]. For example, the second harmonic occurred at 5 GHz, making it difficult to distinguish from the original mixed signal E_4 at 5 GHz. To address this leakage issue, we implemented a dual-mixer configuration with M1 and M2, along with an additional 5.99 GHz RF reference for mixing, as shown in the orange-shaded area of Fig. 2. The Ref served as a common source for both mixing channels. Through heterodyning with the input signals, it generated new frequency components at sum and difference frequencies. This spectral relocation enabled effective separation of target signals from harmonic interference through subsequent filtering, effectively suppressed microwave leakage. Additionally, the phase noise of Ref was canceled out after dual-mixing. The specific process and principles were as follow. Given E_{Ref} expressed as

$$E_{Ref} = \cos\left(\omega_{Ref}t + \varphi_{Ref}\right) \tag{7}$$

where ω_{Ref} and φ_{Ref} represent the angular frequency and initial phase of the signal, respectively. Then, the two output signals from M1 and M2 could be written as

$$E_6 = \cos\left[(3\omega_0 - \omega_{Ref})t + (3\varphi_0 + 3\varphi_{p1} - \varphi_{Ref})\right] \quad (8)$$

$$E_7 = \cos\left[(\omega_{Ref} - \omega_0)t + (\varphi_{Ref} - \varphi_0 - \varphi_{p1} - \varphi_{p2} - \varphi_{p3})\right] \quad (9)$$

When E_6 was mixed with E_7, the output became

$$E_8 = \cos(2\omega_0 t + 2\varphi_0) \quad (10)$$

From the equation (10), the phase noise introduced by Ref had been eliminated during the mixing process. We carefully chose modulation frequencies to ensure that all input frequencies and their harmonics were distinct from the output frequency. The two resulting outputs, E_6 (1.51 GHz) and E_7 (3.49 GHz), were each passed through a bandpass filter before mixing, thereby generating a 5 GHz signal. In this way, the wanted output signal from the mixer at the remote end was well separated from the harmonics of the input signal before we performed the final phase analysis.

4. Results and analysis

To achieve the dissemination stability over the synchronous link, the phase difference between the 2.5 GHz reference signal (E_9) and the 2.5 GHz signal (E_0) from the reference was measured using a phase detector. The resulting phase difference was recorded as a voltage signal $V(t)$, which represents the phase shift over time, utilizing a 7-1/2 digit digital multimeter (Keithley DMM7510). Its measurement bandwidth is 30 Hz, so it will not be affected by the high-frequency signal output by the mixer. By analyzing the phase difference, we obtained the relative time delay between the two 2.5 GHz signals as follows:

$$\Delta t = \frac{1}{\omega_0} arcsin \frac{V(t)}{V_{\mathrm{pp}}/2} \quad (11)$$

here, ω_0 is the angular frequency of the 2.5 GHz transmitted signal, and V_{pp} is the peak-to-peak value of the phase change $V(t)$ within the 2π range. During the measurement of the relative time delay, we compare the outcomes with and without employing the dual-mixer technique. Additionally, to ensure the fidelity of the measurements, background noise tests and free-running tests were carried out. The phase fluctuations from these tests are depicted in Fig. 3.

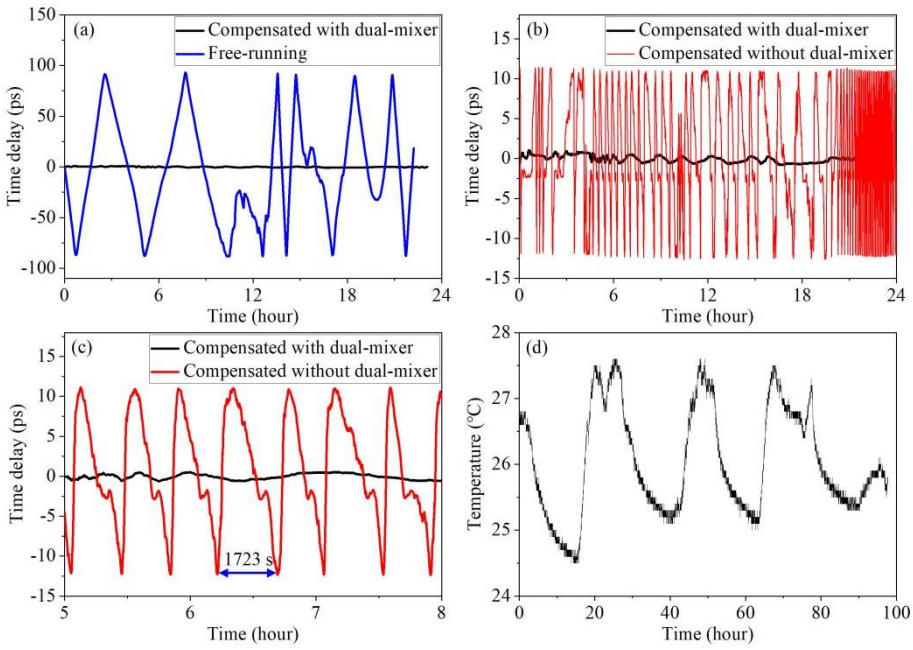

Fig. 3. (a) Relative time delay under free-running (blue) and compensated with dual-mixer (black). (b) Relative time delay under compensation with (black) and without dual-mixer (red). (c) Zoom in data in (b). (d) Temperature changes in the laboratory in duration of four days.

As depicted from Fig. 3(a), the time delay of the signal in free-running mode exhibited periodic variations, which were attributed to the limited phase measurement range of the equipment. The time delay fluctuation for free-running fiber link exceeds 1 ns. However, with the compensation device in place, the time delay fluctuation was confined to within 2 ps. This demonstrates that the delay fluctuations induced by the optical fiber were effectively mitigated. The periodic fluctuations represented by the red line in Fig. 3(b) were a result of the harmonic effect discussed in Section 3. Figure 3(c) shows part of the data from Fig. 3(b), revealing a periodic fluctuation cycle of 1723 seconds, which correlated with the rate of temperature change. To confirm this correlation, we recorded the laboratory's temperature variations during the test, as presented in Fig. 3(d). The temperature changed by approximately 2.5 ℃ every 12 hours. Given the measured effective temperature coefficient of phase delay ($76\,ps/(km\cdot℃)$)[24], the temporal evolution of phase fluctuations for a 2.5 GHz uncompensated signal propagating through 50 km fiber could be expressed as

$$\frac{d\varphi}{dt}=\frac{d\varphi}{dT}\cdot\frac{dT}{dt}=2\pi f\cdot\alpha\cdot L\cdot\frac{dT}{dt}=\frac{47.5}{43200}\pi\ \mathrm{rad/s} \tag{12}$$

The phase cycle period was determined as $2\pi\div(47.5\pi/43200)=1818.95\ \mathrm{s}$,

showing excellent agreement with experimental measurements. The stability of the propagation delay fluctuations indicates that the dual-mixer structure effectively eliminates the impact of microwave leakage.

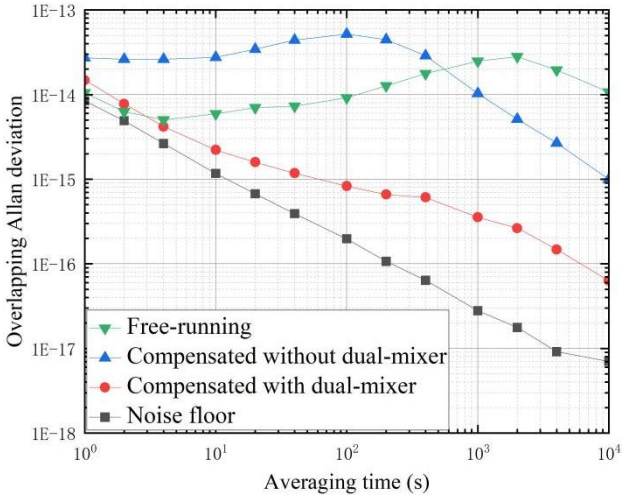

Fig. 4. Overlapping Allan deviation of different frequency transfer system.

The overlapping Allan deviation, calculated according to the phase drift, is shown in Fig. 4. The stability of the free-running system is 1.05×10^{-14} at 1 s gate time and 1.07×10^{-14} at 10^4 s. The blue curve represents the instability of the compensation system without the dual-mixer. The peak observed in the blue curve around 100 s was attributed to periodic phase fluctuations induced by temperature variations. When the dual-mixer was implemented, as indicated by the red curve, this peak was effectively suppressed, and the frequency stability was enhanced by two orders of magnitude at around 100 s. The long-term stability achieved was 6.33×10^{-17} for an averaging time of 10,000 s.

Table 1

Performance comparison with others works.

Reference	Frequency	Distance	Measuring equipment	Short-term stability	Long-term stability
[20]	1 GHz	50 km	——	4.47×10^{-13}@1 s	6.3×10^{-17}@10^4 s
		50 km	——	5.5×10^{-13}@1 s	3.02×10^{-16}@10^4 s
[21]	2 GHz	2 km	7-1/2 digit multimeter	4.2×10^{-15}@1 s	2.5×10^{-17}@10^4 s
		5 km		5.9×10^{-15}@1 s	4.8×10^{-17}@10^4 s

		10 km		6.2×10^{-15}@1 s	7.1×10^{-17}@10^4 s
[26]	1 GHz	50 km 50 km	5125A	3.1×10^{-14}@1 s 3.7×10^{-14}@1 s	2.7×10^{-17}@10^5 s 3.0×10^{-17}@10^5 s
[19]	1 GHz	55 km	8-1/2 digit multimeter	2×10^{-14}@1 s	1.6×10^{-16}@10^4 s
[22]	1 GHz	55 km	5125A	1.3×10^{-14}@1 s	8.1×10^{-18}@10^4 s
Our work	2.5 GHz	50 km	7-1/2 digit multimeter	1.35×10^{-14}@1 s	6.32×10^{-17}@10^4 s

In addition, we compared our work with previously published results related to multiple-access fiber microwave frequency transfer, as presented in Table 1. All the studies listed employed the noise compensation module at the remote end. The implementation of passive compensation in Ref. [20] and [21] enabled the achievement of long-term stability on the order of 10^{-17}, while also significantly reducing system costs. However, since distinct wavelengths were necessary to differentiate each remote site, the long-term stability would degrade as the number of remote sites increased. In our implementation, distinct signals were routed through separate return branches. This configuration prevented spectral overlap between user channels, effectively suppressing group velocity dispersion effects. The dual-mixing scheme exhibited inherent temperature stability, improving the system's long-term stability from 1×10^{-15} to 6.33×10^{-17} (Allan deviation, 10^4 s averaging). The reference signal operated with standard specifications, as its phase noise was suppressed through differential signal processing. Compared with Ref. [26], which used the compensation method involving a phase-locking loop (PLL) and oven-controlled crystal oscillator (OCXO), our dual-mixer approach is expected to further decrease system complexity and cost. Ref. [19] and [22] integrated a scheme for extracting signals from intermediate nodes. To mitigate the impact of backscattering, Ref. [22] employed optical-to-electrical and electrical-to-optical conversions at the local site, achieving a long-term stability of 8.1×10^{-18} at 10^4 s. In contrast, our simplified local structure is more suitable for star-shaped frequency distribution networks. Overall,

our system is straightforward, cost-effective, and possesses high engineering value. Moving forward, we plan to explore the miniaturization of its design.

5. Conclusion

In summary, we proposed a fiber-based radio frequency propagation scheme based on passive phase noise cancellation. The remote simple mixing structure not only facilitates multi-user frequency distribution, but also helps to reduce the cost. By directly reflecting the transmission signal on the corresponding link, we increase scalability while maintaining the symmetry of multi-user dissemination. To address the issue of RF device leakage, we employ a dual-mixer approach to separate different frequencies. The stability of the RF signal reproduced at the remote end, after being transmitted over 50 km, is measured at 1.35×10^{-14} at 1 s and 6.32×10^{-17} at 10^4 s. The results indicate that our scheme features a simple structure and effectively suppresses environmental noise. It offers significant reference value for the engineering of frequency transfer networks extending from central cities to surrounding areas.

CRediT authorship contribution statement

Shi Luo: Writing - original draft, Investigation, Methodology, Data curation. **Zhibin Zhang:** Validation, Methodology, Data curation. **Shun Wu:** Writing - review and editing, Supervision, Funding acquisition, Resources.

Declaration of competing interest

The authors declare that they have no known competing financial interests or personal relationships that could have appeared to influence the work reported in this paper.

Data availability

Data will be made available on request.

Funding

Project supported by the Campus Science Foundation of Wuhan Institute of Technology (grant number 22QD01).

Reference

[1] S.M. Foreman, K.W. Holman, D.D. Hudson, D.J. Jones, J. Ye, Remote transfer of ultrastable frequency references via fiber networks, Review of Scientific Instruments 78 (2007) 021101.

[2] W.M. Campbell, B.T. McAllister, M. Goryachev, E.N. Ivanov, M.E. Tobar, Searching for scalar dark matter via coupling to fundamental constants with photonic, atomic, and mechanical oscillators, Physical Review Letters 126 (2021) 071301.

[3] Y.B. He, K.G.H. Baldwin, B.J. Orr, R.B. Warrington, M.J. Wouters, A.N. Luiten, P. Mirtschin, T. Tzioumis, C. Phillips, J. Stevens, B. Lennon, S. Munting, G. Aben, T. Newlands, T. Rayner, Long-distance telecom-fiber transfer of a radio-frequency reference for radio astronomy, Optica 5 (2018) 138.

[4] K. Grainge, B. Alachkar, S. Amy, *et al.*, Square kilometre array: the radio telescope of the XXI century, Astronomy Reports 61 (2017) 288.

[5] F.X. Wen, H. Wymeersch, 5G synchronization, positioning, and mapping from diffuse multipath, IEEE Wireless Communications Letters 10 (2021) 43.

[6] C. Clivati, R. Aiello, G. Bianco, *et al.*, Common-clock very long baseline interferometry using a coherent optical fiber link, Optica 7 (2020) 1031.

[7] C. Daussy, O. Lopez, A. Amy-Klein, A. Goncharov, M. Guinet, C. Chardonnet, F. Narbonneau, M. Lours, D. Chambon, S. Bize, A. Clairon, G. Santarelli, M.E. Tobar, A.N. Luiten, Long-distance frequency dissemination with a resolution of 10^{-17}, Physical Review Letters 94 (2005) 203904.

[8] B. Wang, C. Gao, W.L. Chen, J. Miao, X. Zhu, Y. Bai, J.W. Zhang, Y.Y. Feng, T.C. Li, L.J. Wang, Precise and continuous time and frequency synchronisation at the 5×10^{-19} accuracy level, Scientific Reports 2 (2012) 556.

[9] M. Fujieda, M. Kumagai, T. Gotoh, M. Hosokawa, Ultrastable frequency dissemination via optical fiber at NICT, IEEE Transactions on Instrumentation and Measurement 58 (2009) 1223.

[10] L.S. Ma, P. Jungner, J. Ye, J.L. Hall, Delivering the same optical frequency at two places: accurate cancellation of phase noise introduced by an optical fiber or other time-varying path, Optics Letters 19 (1994) 1777.

[11] J.Y. Han, C.X. Liu, S. Yu, T.W. Jiang, S.J. Zhou, J.M. Shang, Y.J. Qiao, Stable radio frequency dissemination-based on passive method by avoiding second harmonic distortion, Optical Engineering 58 (2019) 1.

[12] C. Gao, B. Wang, W. Chen, Y. Bai, J. Miao, X. Zhu, T. Li, L.J. Wang, Fiber-based multiple-access ultrastable frequency dissemination, Optics Letters 37 (2012) 4690.
[13] J.B. Ajo-Franklin, S. Dou, N.J. Lindsey, I. Monga, C. Tracy, M. Robertson, V. Rodriguez Tribaldos, C. Ulrich, B. Freifeld, T. Daley, X. Li, Distributed acoustic sensing using dark fiber for near-surface characterization and broadband seismic event detection, Scientific Reports 9 (2019) 1328.
[14] M. Fujieda, M. Kumagai, S. Nagano, Coherent microwave transfer over a 204-km telecom fiber link by a cascaded system, IEEE Transactions on Ultrasonics, Ferroelectrics, and Frequency Control 57 (2009) 168.
[15] W.X. Xue, H.L. Quan, W.Y. Zhao, S.G. Zhang, Microwave frequency transfer over a 500-km cascaded fiber link using tracking filter, Optics & Laser Technology 163 (2023) 109327.
[16] Q. Li, L. Hu, J.B. Zhang, J.P. Chen, G.L. Wu, Fiber radio frequency transfer using bidirectional frequency division multiplexing dissemination, IEEE Photonics Technology Letters 33 (2021) 660.
[17] H. Gao, B.D. Zhao, Z.Z. Zhao, J.H. Cheng, C.X. Liu, Z.Y. Chen, T.W. Jiang, B. Luo, S. Yu, H. Guo, Multi-nodes dissemination of stable radio frequency with 10^{-17} instability over 2000 km optical fiber, Optics Express 31 (2023) 25598.
[18] H.W. Li, G.L. Wu, J.P. Zhang, J.G. Shen, J.P. Chen, Multi-access fiber-optic radio frequency transfer with passive phase noise compensation, Optics Letters 41 (2016) 5672.
[19] X. Zhu, B. Wang, C. Gao, L.J. Wang, Fiber-based multiple-access frequency synchronization via 1f–2f dissemination, Chinese Physics B 25 (2016) 090601.
[20] L.Q. Yu, R. Wang, L. Lu, Y. Zhu, J.L. Zheng, C.X. Wu, B.F. Zhang, P.Z. Wang, WDM-based radio frequency dissemination in a tree-topology fiber optic network, Optics Express 23 (2015) 19783.
[21] Y. Bai, B. Wang, C. Gao, J. Miao, X. Zhu, L.J. Wang, Fiber-based radio frequency dissemination for branching networks with passive phase-noise cancelation, Chinese Optics Letters 13 (2015) 061201.
[22] M.Y. Jiang, Y.Q. Chen, N. Cheng, Y.G. Sun, J.L. Wang, R. Wu, F. Yang, H.W. Cai, Y.Z. Gui, Multi-access RF frequency dissemination based on round-trip three-wavelength optical compensation technique over fiber-optic link, IEEE Photonics Journal 11 (2019) 1.
[23] S.S. Yu, H.L. Quan, W.Y. Zhao, W.X. Xue , X. Wang, S.G. Zhang, Multi-access fiber microwave frequency transmission technology, Acta Optica Sinica 44 (2024) 0506001.
[24] X. Zhu, B. Wang, Y.C. Guo, Y.B. Yuan, R. Gamatham, B. Wallace, K. Grainge, L.J. Wang, Robust fiber-based frequency synchronization system immune to strong temperature fluctuation, Chinese Optics Letters 16 (2018) 010605.
[25] S.J. Zhou, C.X. Liu, X. Chen, T.W. Jiang, J.T. Cong, H. Gao, B. Luo, S. Yu, Stable RF transmission in dynamic phase correction with Rayleigh backscattering noise suppression, Optical Fiber Technology 56 (2020) 102165.

[26] B. Wang, X. Zhu, C. Gao, Y. Bai, J.W. Dong, L.J. Wang, Square kilometre array telescope-precision reference frequency synchronisation via 1f-2f dissemination, Scientific Reports 5 (2015) 13851.